Rapid Communications

Dyakonov-like waveguide modes in an interfacial strip waveguide

E. V. Anikin,[1,*] D. A. Chermoshentsev,[2] S. A. Dyakov,[1,†] and N. A. Gippius[1]
[1]*Skolkovo Institute of Science and Technology, 143025 Moscow Region, Russia*
[2]*Skolkovo Institute of Science and Technology, 143025 Moscow Region, Russia;*
Moscow Institute of Physics and Technology, 141701 Institutskiy pereulok 9, Moscow Region, Russia;
and Russian Quantum Center, Skolkovo, Moscow 143025, Russia

(Received 27 July 2020; revised 24 September 2020; accepted 29 September 2020; published 19 October 2020)

We study Dyakonov surface waveguide modes in a waveguide represented by an interface of two anisotropic media confined between two air half-spaces. We analyze such modes in terms of perturbation theory in the approximation of weak anisotropy. We show that in contrast to conventional Dyakonov surface waves that decay monotonically with distance from the interface, Dyakonov waveguide modes can have local maxima of the field intensity away from the interface. We confirm our analytical results by comparing them with full-wave electromagnetic simulations. We believe that this work can bring new ideas in the research of Dyakonov surface waves.

DOI: 10.1103/PhysRevB.102.161113

Surface electromagnetic waves are solutions of Maxwell's equations in the form of monochromatic waves, which propagate along the interface of two dissimilar media and decay in the directions perpendicular to the interface. Examples of surface waves include surface plasmon polaritons at a metal-dielectric interface [1], Tamm surface states at a photonic crystal boundary [2–4], surface solitons at a nonlinear interface [5], and many others. A special case of surface waves is Dyakonov surface waves (DSWs) supported at the interface of two materials, at least one of which is anisotropic. Since the discovery in 1988 by Dyakonov [6], extensive research has been performed toward the theoretical study and experimental realization of DSWs and finding optimal material and geometrical configurations, which would be most suitable for potential practical implementations. Different combinations of isotropic, uniaxial, biaxial, and chiral materials have been demonstrated to support DSWs at their interfaces [4,7–20]. The first experimental observation of DSWs using the prism coupling method was reported in 2009 by Takayama *et al.* [21]. Due to naturally small anisotropy of birefringent media, DSWs exist only in a narrow range of angular directions parallel to the interface plane. Wider DSW existence regions can be achieved using ultrathin partnering nanolayers, which can substantially release the Dyakonov condition and simplify DSW experimental observation [22,23]. Yet another realization of DSWs has been demonstrated theoretically and experimentally for metamaterials with artificially designed shape anisotropy [23–30].

In contrast to surface plasmon-polaritons and many other surface waves, DSWs can exist at the interface of two dielectrics. It means that DSWs potentially have no theoretical limit in propagation length. In this sense, a study of DSW propagation in a corresponding waveguide would be interesting for the theory of nanophotonics and also rather intriguing from a practical viewpoint. Recently, waveguide properties of DSWs on cylindrical surfaces have been demonstrated in Ref. [31]. Due to the bending of the waveguide boundary, such DSWs have inevitable radiative losses, which tend to zero when the cylinder diameter tends to infinity.

In this Rapid Communication, we consider a waveguide for DSWs represented by a strip of the interface between two identical uniaxial birefringent dielectrics. We will demonstrate that such a flat waveguide can guide DSWs without losses.

The schematic of the waveguide for DSWs is shown in Fig. 1. It consists of two anisotropic dielectric slabs separated from air by planes $|y| = d/2$. The slabs have width d in the y direction, are infinite in the x direction, and semi–infinite in the z direction. These two dielectrics have different orientations of optical axes, and there is an interface between them at the plane $z = 0$. Although we are mostly interested in the case of two uniaxial media, we extend our scope to consideration of biaxial crystals with similar dielectric tensors whose axes are rotated by 45° with respect to the initial coordinate system. Thus, the dielectric tensor inside the structure (at $|y| < d/2$) has the form

$$\hat{\epsilon}(z) = \hat{\epsilon}_0 + \delta\hat{\epsilon}(z), \quad \hat{\epsilon}_0 = \mathrm{diag}(\epsilon_1, \epsilon_1, \epsilon_2),$$
$$\delta\hat{\epsilon}(z) = \mathrm{sign}(z)\begin{pmatrix} 0 & \delta\epsilon & 0 \\ \delta\epsilon & 0 & 0 \\ 0 & 0 & 0 \end{pmatrix}. \tag{1}$$

We treat the parameters $\epsilon_{1,2}$ and $\delta\epsilon$ as independent ones. However, by setting $\epsilon_1 - \epsilon_2 = \delta\epsilon$, one can consider the case of two uniaxial crystals. Please note that such a representation of dielectric tensor $\hat{\epsilon}$ is possible only for the optical axes rotation angles of ±45° relative to the x axis.

In such a structure, lossless modes propagating along the x axis can exist, which are localized in the z direction near the

*evgenii.anikin@skoltech.ru
†s.dyakov@skoltech.ru

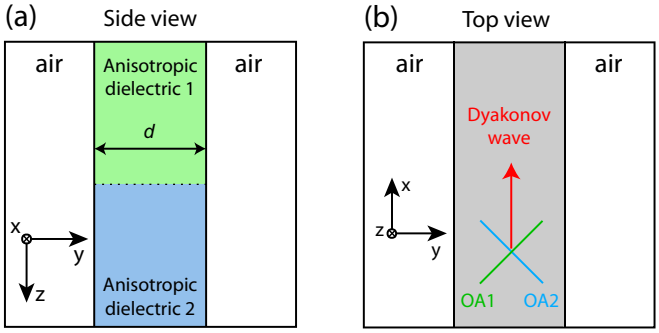

FIG. 1. (a) Side view and (b) top view of Dyakonov waveguide. Optical axes (OAs) of anisotropic dielectrics 1 and 2 are perpendicular to each other and form the angle of 45° to the waveguide boundaries.

interface of two slabs. We will call them Dyakonov waveguide modes (DWMs). DWMs can be analyzed in the framework of perturbation theory by the nondiagonal part of the permittivity tensor. Without perturbation, the waveguide is translationally invariant in both x and z directions and all eigenmodes have the form of plane waves $\vec{E}_{k_x,k_z}(y)e^{ik_x x+ik_z z}$, where k_x and k_z are the projections of the wave vector $\vec{k}$. When the perturbation is present, a DWM can appear with a lower frequency than all waveguide modes at a fixed k_x. For weak perturbation, the DWM decays slowly away from the interface. Because of this, it is possible to describe DWMs in terms of unperturbed waveguide modes multiplied by a slowly varying envelope.

The general solution for waveguide modes in an anisotropic waveguide with permittivity $\hat{\epsilon}_0$ can be obtained analytically for arbitrary k_x and k_z (see Supplemental Material in Ref. [32]). For waves propagating in the x direction, the modes are identical to those of an isotropic waveguide, i.e., they have the same fields and frequency. Namely, the modes with $\vec{E} \parallel Oz$ coincide with Transverse Electric (TE) modes of an isotropic waveguide with permittivity ϵ_2, and the modes with $\vec{E} \perp Oz$ coincide with Transverse Magnetic (TM) modes of an isotropic waveguide with permittivity ϵ_1. For $\epsilon_2 < \epsilon_1$, the two lowest waveguide modes intersect [have the same frequency ω, see Fig. 2(a)] at some value of propagation constant k_x. Thus, both of them should be taken into account in the decomposition of DWMs over waveguide eigenmodes.

Close to the intersection of fundamental TE and TM modes, the nondiagonal perturbation $\delta\hat{\epsilon}$ leads to considerable mixing of them. Moreover, the contribution of all other modes can be neglected, provided that the mode spacing (which has order c/d) is much larger than the distance between the two lowest modes.

We consider Maxwell's equations as an eigenvalue problem,

$$c^2 \mathrm{rotrot}\vec{E} = \omega^2 \hat{\epsilon}\vec{E}, \tag{2}$$

where ω is the frequency of electromagnetic oscillations and c is the speed of light. All eigenmodes of this problem constitute a basis in the space of fields. As the unperturbed problem has translational symmetry in z direction, we will consider the basis

$$\vec{\mathcal{E}}^n_{k_x,k_z}(y,z) = \vec{E}^n_{k_x,k_z}(y)e^{ik_z z}, \tag{3}$$

with corresponding eigenvalues $\omega_{k_x,k_z,n}$, where n is the index enumerating different modes. The set of all modes at particular k_x, k_z includes a finite number of waveguide modes which decay exponentially away from the waveguide and a continuum of free-space modes corresponding to plane-wave scattering on the waveguide. Below, we don't take the continuum modes into account because, as will be shown, only the modes with lowest frequencies contribute to DWMs, and the expansion including lowest TE and TM modes reads

$$\vec{E}(y,z) = \int \frac{dk_z}{2\pi}\left[\alpha(k_z)\vec{\mathcal{E}}^{\mathrm{TE}}_{k_x,k_z} + \beta(k_z)\vec{\mathcal{E}}^{\mathrm{TM}}_{k_x,k_z}\right]. \tag{4}$$

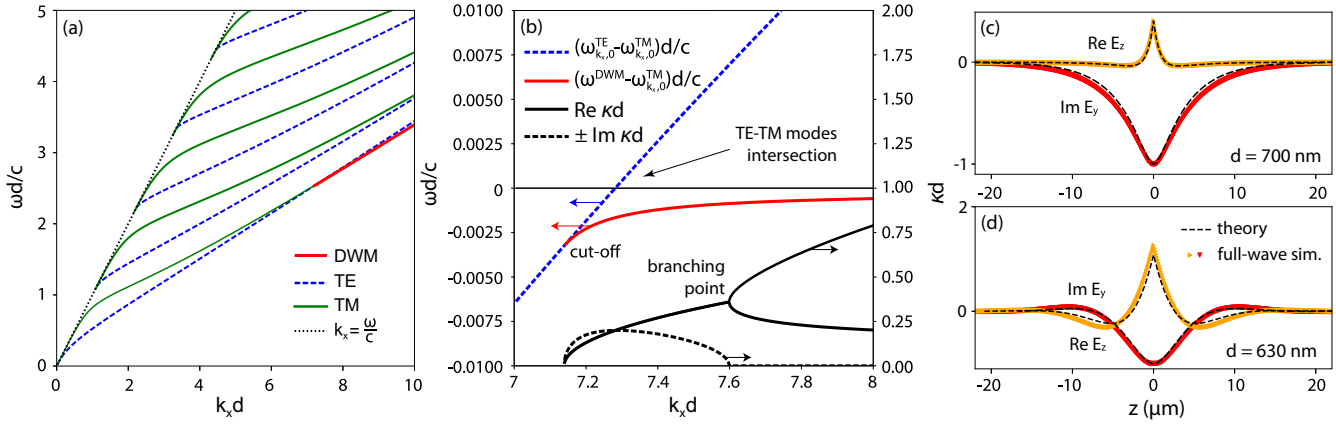

FIG. 2. (a) The dispersions of the DWM (red solid line) and the TE and TM modes of an anisotropic waveguide (blue dashed line and green solid line) with permittivity $\hat{\epsilon}_0$ traveling along x axis. (b) The in-plane wave-vector dependence of the real and imaginary parts of the decay constants $\kappa_{1,2}$ (black solid and dashed line). The dispersions of the DWM (red line) and the TE waveguide mode of an anisotropic waveguide (blue dashed line) with permittivity $\hat{\epsilon}_0$ shown as a difference with the dispersion of the TM waveguide mode. In the presented diagram, the TM waveguide mode corresponds to the horizontal line $\omega d/c = 0$ (black thin solid line). (c), (d) Theoretically calculated fields $E_y(0,z)$ and $E_z(0,z)$ (black dashed lines) shown together with COMSOL simulation results (red and yellow lines) for $\lambda = 1550$ nm and (c) $k_x d = 7.262$, $d = 700$ nm, (d) $k_x d = 8.1938$, $d = 630$ nm. All calculations are made for $\delta\epsilon = 0.5$, $\epsilon_1 = 9.5$, $\epsilon_2 = 9$.

Taking into account the orthogonality of eigenvectors of the eigenvalue problem Eq. (2), we normalize the waveguide modes by a condition

$$\int \left(\vec{\mathcal{E}}^{n}_{k_x,k_z}, \hat{\epsilon}_0 \vec{\mathcal{E}}^{n'}_{k_x,k_z'}\right) dydz = 2\pi\delta(k_z - k_z')\delta_{nn'}. \tag{5}$$

Below we obtain the equation for the envelopes $\alpha(k_z)$ and $\beta(k_z)$. Due to small $\delta\epsilon$, DWMs should have a slow field dependence on z and, hence, the field envelopes $\alpha(k_z)$ and $\beta(k_z)$ are significant only at small k_z. After substituting this expansion in Maxwell equations and taking scalar product of both sides of these equations by $\vec{\mathcal{E}}^{\mathrm{TE}}_{k_x,k_z}$ and $\vec{\mathcal{E}}^{\mathrm{TM}}_{k_x,k_z}$, one obtains

$$\begin{aligned}
\gamma^{\mathrm{TE}}_{k_x,k_z}\alpha(k_z) &= \omega^2 \int \frac{dk_z'}{(2\pi)}\beta(k_z')\langle\vec{\mathcal{E}}^{\mathrm{TE}}_{k_x,k_z}\delta\hat{\epsilon}\vec{\mathcal{E}}^{\mathrm{TM}}_{k_x,k_z'}\rangle,\\
\gamma^{\mathrm{TM}}_{k_x,k_z}\beta(k_z) &= \omega^2 \int \frac{dk_z'}{(2\pi)}\alpha(k_z')\langle\vec{\mathcal{E}}^{\mathrm{TM}}_{k_x,k_z}\delta\hat{\epsilon}\vec{\mathcal{E}}^{\mathrm{TE}}_{k_x,k_z'}\rangle,
\end{aligned} \tag{6}$$

where $\gamma^{\mathrm{TE(TM)}}_{k_x,k_z} = (\omega^{\mathrm{TE(TM)}}_{k_xk_z})^2 - \omega^2$.

The matrix elements $\langle\vec{\mathcal{E}}^{\mathrm{TE}}_{k_x,k_z}\delta\hat{\epsilon}\vec{\mathcal{E}}^{\mathrm{TE}}_{k_x,k_z'}\rangle$ and $\langle\vec{\mathcal{E}}^{\mathrm{TM}}_{k_x,k_z}\delta\hat{\epsilon}\vec{\mathcal{E}}^{\mathrm{TM}}_{k_x,k_z'}\rangle$ are not present in Eqs. (6) because they turn out to be zero due to symmetry properties of TE and TM modes. Also, at small wave vectors, the matrix element corresponding to mixing between TE and TM modes $\langle\vec{\mathcal{E}}^{\mathrm{TE}}_{k_x,k_z}\delta\hat{\epsilon}\vec{\mathcal{E}}^{\mathrm{TM}}_{k_x,k_z'}\rangle$ reads

$$\begin{aligned}
\langle\vec{\mathcal{E}}^{\mathrm{TE}}_{k_x,k_z}\delta\hat{\epsilon}\vec{\mathcal{E}}^{\mathrm{TM}}_{k_x,k_z'}\rangle &= 2i\mathcal{P}\left(\frac{1}{k_z - k_z'}\right)k_z\delta\epsilon\sigma,\\
\sigma\delta\epsilon &= \int_{-a/2}^{a/2} dy\left(\partial_{k_z}\vec{E}^{\mathrm{TE}}_{k_x,k_z}(y)\delta\hat{\epsilon}\vec{E}^{\mathrm{TM}}_{k_x,k_z'}(y)\right)\big|_{k_z,k_z'=0},
\end{aligned} \tag{7}$$

where $\mathcal{P}$ denotes the principal value. After substituting Eqs. (7) to (6) and performing the inverse Fourier transform of Eqs. (6), one gets a system of Ordinary differential equations in coordinate space for Fourier images of $\alpha(k_z)$ and $\beta(k_z)$, $\alpha(z)$ and $\beta(z)$.

Expanding the frequencies of TE and TM modes in k_z up to quadratic terms, one gets

$$\begin{pmatrix} \gamma^{\mathrm{TE}}_{k_x,0} - \frac{1}{2m_1}\frac{\partial^2}{\partial z^2} & i\omega^2\sigma\delta\epsilon\partial_z\mathrm{sign}(z) \\ i\omega^2\sigma\delta\epsilon\,\mathrm{sign}(z)\partial_z & \gamma^{\mathrm{TM}}_{k_x,0} - \frac{1}{2m_2}\frac{\partial^2}{\partial z^2} \end{pmatrix}\begin{pmatrix}\alpha(z)\\ \beta(z)\end{pmatrix} = 0, \tag{8}$$

where all the coefficients in Eq. (8) are expressed through the quantities referring to the planar waveguide,

$$m^{-1}_{1(2)} = \frac{\partial^2}{\partial k_z^2}\left(\omega^{\mathrm{TE(TM)}}_{k_x,k_z}\right)^2\big|_{k_z=0}, \tag{9}$$

and σ is defined by Eq. (7). The system Eq. (8) has solutions in the form of decaying exponential functions for $z > 0$ and $z < 0$ which can be matched using the boundary conditions at $z = 0$. These exponentially decaying solutions exactly correspond to DWMs localized near the interface with field distributions given by Eq. (4). By integrating Eq. (8) in the neighborhood of $z = 0$, one gets that $\partial_z\beta(z)$ is continuous, and the condition for $\partial_z\alpha(z)$ reads

$$\partial_z\alpha(+0) - \partial_z\alpha(-0) = 4im_1\omega^2\sigma\delta\epsilon\beta(0). \tag{10}$$

The explicit expressions for coefficients Eq. (9) in the effective equation for envelopes Eq. (8) can be easily calculated numerically. They also drastically simplify in the limit when $\epsilon_1 - \epsilon_2 \ll \epsilon_1$ and all modes are very close to that of the planar isotropic waveguide. In this limit, fundamental TE and TM modes intersect at $k_xd \gg 1$. So, one can utilize the large wave-vector expansion of $\omega^{\mathrm{TE}}_{k_x,0}$ and $\omega^{\mathrm{TM}}_{k_x,0}$ to find the intersection point. The resulting wave vector of intersection reads

$$k_xd \approx \sqrt{\epsilon_1}\left(\frac{2\pi^2\sqrt{\epsilon_1 - 1}}{\epsilon_1(\epsilon_1 - \epsilon_2)}\right)^{\frac{1}{3}}. \tag{11}$$

At large k_x, the parameters m_1^{-1} and m_2^{-1} approach c^2/ϵ_1, and the asymptotic behavior of the matrix element is $\sigma = (k_x\epsilon_1)^{-1}$.

The examination of the system Eq. (8) allows finding the domain of existence, the dispersion law, and the field structure of DWMs. Before we go into further detail, let us emphasize that such modes propagate along the x axis completely without losses. This is because, as shown below, the frequencies of DWMs in such a structure are lower than the frequencies of the waveguide modes. Thus, DWMs cannot scatter into waveguide modes or free-space modes without violation of energy or momentum conservation law. Therefore, the imaginary parts of the frequency and the wave vector are exactly zero, $\omega'' = 0$ and $k_x'' = 0$.

The exponentially decaying solution of Eq. (8) obeying the boundary conditions reads

$$\begin{aligned}
\alpha(z) &= \frac{\omega^2\sigma\delta\epsilon e^{-\kappa_2|z|}}{\left(\gamma^{\mathrm{TE}}_{k_x,0} - \frac{\kappa_2^2}{2m_1}\right)} - \frac{\omega^2\sigma\delta\epsilon e^{-\kappa_1|z|}}{\left(\gamma^{\mathrm{TE}}_{k_x,0} - \frac{\kappa_1^2}{2m_1}\right)},\\
\beta(z) &= -i\left(\frac{e^{-\kappa_2|z|}}{\kappa_2} - \frac{e^{-\kappa_1|z|}}{\kappa_1}\right),
\end{aligned} \tag{12}$$

where $\kappa_{1,2}$ are two roots with positive real part of the characteristic equation:

$$\left(\gamma^{\mathrm{TE}}_{k_x,0} - \frac{\kappa^2}{2m_1}\right)\left(\gamma^{\mathrm{TM}}_{k_x,0} - \frac{\kappa^2}{2m_2}\right) + \omega^4\sigma^2\delta\epsilon^2\kappa^2 = 0. \tag{13}$$

The implicit dispersion follows from boundary conditions and has the form

$$\sqrt{m_1m_2\gamma^{\mathrm{TE}}_{k_x,0}\gamma^{\mathrm{TM}}_{k_x,0}} = 2m_1m_2(\omega^2\sigma\delta\epsilon)^2 - m_2\gamma^{\mathrm{TM}}_{k_x,0}. \tag{14}$$

Whether there exists a solution for these equations depends on the relation between $\omega^{\mathrm{TE}}_{k_x,0}$ and $\omega^{\mathrm{TM}}_{k_x,0}$ and the off-diagonal matrix element. In particular, the solution of Eq. (14) exists when the lower cutoff condition is satisfied [see red curve in Fig. 2(b)]:

$$\left(\omega^{\mathrm{TM}}_{k_x,0}\right)^2 - \left(\omega^{\mathrm{TE}}_{k_x,0}\right)^2 \leqslant 2m_1\left(\omega^{\mathrm{TE}}_{k_x,0}\right)^4\sigma^2\delta\epsilon^2. \tag{15}$$

From expressions Eqs. (12)–(14), one can see that the decay constants $\kappa_{1,2}$ can be either complex and conjugate to each other or both real. The case of complex $\kappa_{1,2}$ implements near the vicinity of the TE and TM mode intersection, whereas far enough from the intersection point, both κ_1 and κ_2 are real. These alternatives are separated by the branching point where two roots of the characteristic Eq. (13) coincide. As the DWMs are qualitatively different for these two cases, let us consider them in more detail.

First, we consider a large separation between TE and TM modes. In this case, for the solutions of the characteristic equation and the field distributions, simple asymptotic

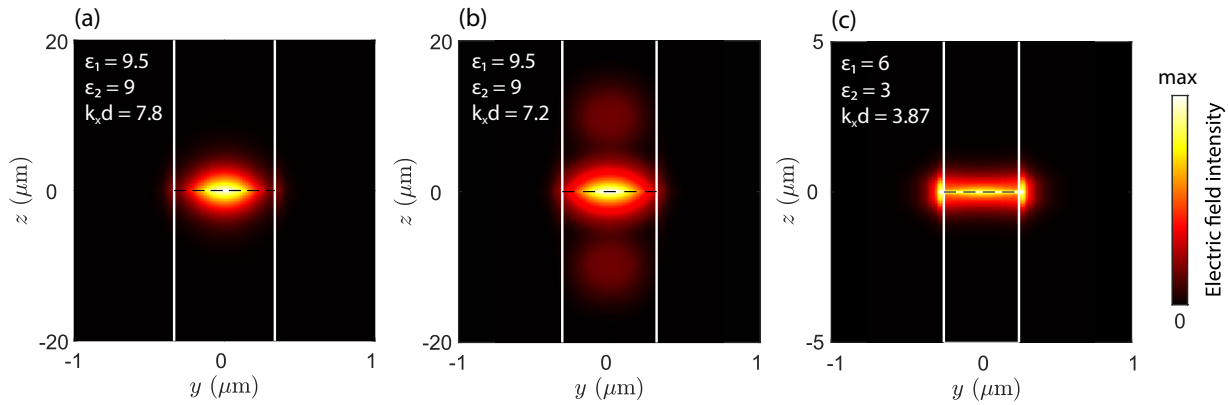

FIG. 3. Electric field intensity in DWMs at $\lambda = 1.55\ \mu$m and (a) $\varepsilon_1 = 9.5, \varepsilon_2 = 9, k_x d = 7.8, d \approx 670$ nm; (b) $\varepsilon_1 = 9.5, \varepsilon_2 = 9, k_x d = 7.2, d \approx 625$ nm; (c) $\varepsilon_1 = 6, \varepsilon_2 = 3, k_x d \approx 3.87, d = 500$ nm. White vertical lines denote the waveguide boundaries, black dashed horizontal lines denote the interface between anisotropic dielectrics.

expressions can be obtained. Thereby, the DWM frequency evaluated from Eq. (14) is very close to TM mode frequency:

$$\delta\omega = \omega^{\mathrm{TM}}_{k_x,0} - \omega^{\mathrm{DWM}} \approx \frac{2m_1 m_2 \left(\omega^{\mathrm{TM}}_{k_x,0}\right)^7 \sigma^4 \delta\epsilon^4}{\left(\omega^{\mathrm{TE}}_{k_x,0}\right)^2 - \left(\omega^{\mathrm{TM}}_{k_x,0}\right)^2} \propto \delta\epsilon^4. \quad (16)$$

Also, the amplitudes of TE and TM modes in this limit take the form

$$\alpha(z) = \frac{2m_1 \left(\omega^{\mathrm{TM}}_{k_x,0}\right)^2 \sigma\, \delta\epsilon}{\kappa_1} e^{-\kappa_1 |z|}, \quad \beta(z) = -ie^{-\kappa_2 |z|}, \quad (17)$$

where the decay constants read $\kappa_1^2 \approx 2m_1[(\omega^{\mathrm{TE}}_{k_x,0})^2 - (\omega^{\mathrm{TM}}_{k_x,0})^2]$ and $\kappa_2^2 \approx 4m_2\omega^{\mathrm{TM}}_{k_x,0}\delta\omega$. Thus, in the considered limits, the main contribution to DWMs is from the TM waveguide mode. Its amplitude slowly decays with the decay length $\sim 1/\kappa_2$ [Fig. 3(a)], whereas the amplitude of the TE mode is small by $\delta\epsilon$, and the TE mode is localized near the interface on a much shorter length $\sim 1/\kappa_1$. The theoretically calculated profiles of E_y and E_z for the considered case demonstrate excellent agreement with the results of full-wave electromagnetic simulations of DWMs made in COMSOL [Fig. 2(c)].

Now let us analyze the vicinity of TE and TM mode intersections when the approximation of Eqs. (16) and (17) becomes invalid. The exact solution of Eqs. (12)–(14) should be utilized in this case, and the contributions of TE and TM modes to DWMs as well as the inverse decay lengths κ_1 and κ_2, become comparable. Also, the difference between DWM frequency and the lowest TM mode frequency $\delta\omega$ becomes proportional to $\delta\epsilon^2$, so the separation between DWM and waveguide modes is maximal near the TE and TM mode intersection. As it was stated before, the inverse decay lengths κ_1 and κ_2 acquire nonzero imaginary part closely to the modes intersection [see Fig. 2(b)], so the fields exhibit oscillations with z which results in additional local maxima of the field intensity at some distance from the interface [see Figs. 2(d) and Fig. 3(b)]. This distinct feature distinguishes DWMs from conventional DSWs which exist at the infinite flat interface and decay monotonically.

It should be emphasized once again that the two-mode approximation is valid only provided that the difference between TE and TM mode frequencies is much less then the mode spacing, $\omega^{\mathrm{TE}}_{k_x,0} - \omega^{\mathrm{TM}}_{k_x,0} \ll \frac{\pi^2}{k_x d^2 \epsilon_{1,2}}$. As $\omega^{\mathrm{TE}}_{k_x,0} - \omega^{\mathrm{TM}}_{k_x,0}$ grows with k_x, the two–mode approximation cannot be applied far from the mode intersection point. The above analytical considerations only apply to the case of a small anisotropy $\delta\varepsilon \ll \varepsilon_1, \varepsilon_2$. Properties of DWMs in a more general case of an arbitrary anisotropy, their domain of existence, and the presence of a branching point are subjects of separate research. However, in Fig. 3(c), we show an example of the DWM obtained numerically in COMSOL for $\varepsilon_1 = 6$ and $\varepsilon_2 = 3$. One can see that the electric field intensity decays with distance from the interface even faster than in the considered cases of small anisotropy.

Finally, the considered DWMs can be generalized to a non-45° rotation of optical axes as well as to other types of partnering media, including different combinations of isotropic, uniaxial, biaxial, chiral materials, and also photonic crystals. Existence of DWMs in each particular case is a subject of separate research.

In conclusion, we have analytically and numerically demonstrated the existence of DWMs which can propagate without losses at the interface of two anisotropic dielectric waveguides. On the dispersion diagram, DWMs exist near the intersection of the lowest TE and TM modes of these waveguides. We have shown that DWMs are generally localized on the interface but, under certain conditions, they also may have additional local maxima of the field intensity at some distance from the interface.

This work was supported by the Russian Foundation for Basic Research (Grant No. 18-29-20032).

[1] V. M. Agranovich and D. L. Mills, *Surface Polaritons* (North-Holland Publishing Company, Amsterdam, New York, Oxford, 1982).

[2] A. P. Vinogradov, A. V. Dorofeenko, S. G. Erokhin, M. Inoue, A. A. Lisyansky, A. M. Merzlikin, and A. B. Granovsky, Phys. Rev. B **74**, 045128 (2006).

[3] S. A. Dyakov, A. Baldycheva, T. S. Perova, G. V. Li, E. V. Astrova, N. A. Gippius, and S. G. Tikhodeev, Phys. Rev. B **86**, 115126 (2012).
[4] C. Zhou, T. G. Mackay, and A. Lakhtakia, Optik **211**, 164575 (2020).
[5] Y. V. Kartashov, L. Torner, and V. A. Vysloukh, Phys. Rev. Lett. **96**, 073901 (2006).
[6] M. I. Dyakonov, Sov. Phys. JETP **67**, 714 (1988).
[7] N. Averkiev and M. Dyakonov, Opt. Spectrosc. **68**, 1118 (1990).
[8] O. Takayama, A. Y. Nikitin, L. Martin-Moreno, L. Torner, and D. Artigas, Opt. Express **19**, 6339 (2011).
[9] J. Gao, A. Lakhtakia, and M. Lei, Phys. Rev. A **81**, 013801 (2010).
[10] K. Agarwal, J. A. Polo Jr, and A. Lakhtakia, J. Opt. A: Pure Appl. Opt. **11**, 074003 (2009).
[11] J. A. Polo Jr, S. R. Nelatury, and A. Lakhtakia, JOSA A **24**, 2974 (2007).
[12] T. Repän, O. Takayama, and A. V. Lavrinenko, Photonics **7**, 34 (2020).
[13] Y. Zhang, X. Wang, D. Zhang, S. Fu, S. Zhou, and X.-Z. Wang, Opt. Express **28**, 19205 (2020).
[14] S. Fu, S. Zhou, Q. Zhang, and X. Wang, Opt. Laser Technol. **125**, 106012 (2020).
[15] S. Y. Karpov, Phys. Status Solidi (b) **256**, 1800609 (2019).
[16] Y. Li, J. Sun, Y. Wen, and J. Zhou, Phys. Rev. Appl. **13**, 024024 (2020).
[17] I. Fedorin, Opt. Quantum Electron. **51**, 201 (2019).
[18] A. G. Ardakani, M. Naserpour, and C. J. Zapata-Rodríguez, Photon. Nanostruct.-Fundam. Appl. **20**, 1 (2016).
[19] M. Moradi and A. R. Niknam, Opt. Lett. **43**, 519 (2018).
[20] E. E. Narimanov, Phys. Rev. A **98**, 013818 (2018).
[21] O. Takayama, L. Crasovan, D. Artigas, and L. Torner, Phys. Rev. Lett. **102**, 043903 (2009).
[22] O. Takayama, D. Artigas, and L. Torner, Nat. Nanotechnol. **9**, 419 (2014).
[23] J. Sorni, M. Naserpour, C. Zapata-Rodríguez, and J. Miret, Opt. Commun. **355**, 251 (2015).
[24] D. Artigas and L. Torner, Phys. Rev. Lett. **94**, 013901 (2005).
[25] O. Takayama, E. Shkondin, A. Bodganov, M. E. Aryaee Panah, K. Golenitskii, P. Dmitriev, T. Repan, R. Malureanu, P. Belov, F. Jensen *et al.*, ACS Photon. **4**, 2899 (2017).
[26] S. Jahani and Z. Jacob, Nat. Nanotechnol. **11**, 23 (2016).
[27] O. Takayama, D. Artigas, and L. Torner, Opt. Lett. **37**, 4311 (2012).
[28] V. Kajorndejnukul, D. Artigas, and L. Torner, Phys. Rev. B **100**, 195404 (2019).
[29] O. Takayama, A. A. Bogdanov, and A. V. Lavrinenko, J. Phys.: Condens. Matter **29**, 463001 (2017).
[30] O. Takayama, P. Dmitriev, E. Shkondin, O. Yermakov, M. Panah, K. Golenitskii, F. Jensen, A. Bogdanov, and A. Lavrinenko, Semiconductors **52**, 442 (2018).
[31] K. Y. Golenitskii and A. A. Bogdanov, Phys. Rev. B **101**, 165434 (2020).
[32] See Supplemental Material at http://link.aps.org/supplemental/10.1103/PhysRevB.102.161113 for the analytical solution for waveguide modes in an anisotropic waveguide.